

Structural Health Evaluation of Composite Materials using Lamb Wave Methods

Seth S. Kessler, Ph.D. – Metis Design Corporation

Christopher T. Dunn, Ph.D. – MIT Aero/Astro



Mechanical Design • Composites Engineering • SHM
<http://www.MetisDesign.com>



Technology Laboratory for Advanced Composites
Department of Aeronautics and Astronautics
Massachusetts Institute of Technology



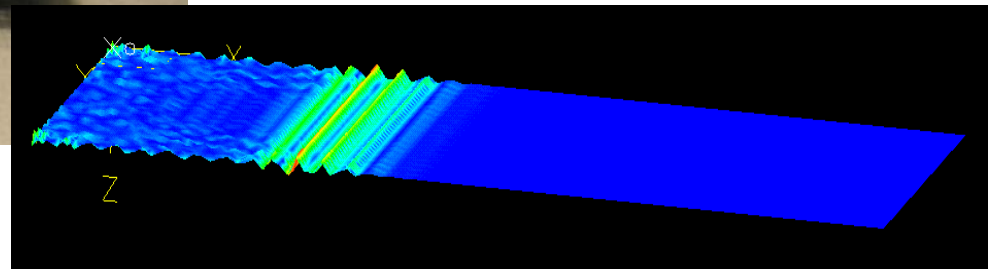
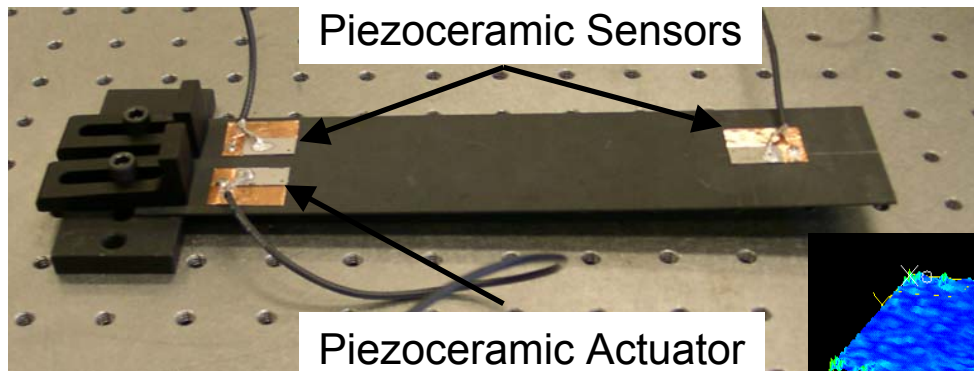
National Reconnaissance Office
Office of Space Launch
Contract #: NRO000-02-C-0625

Program Goals

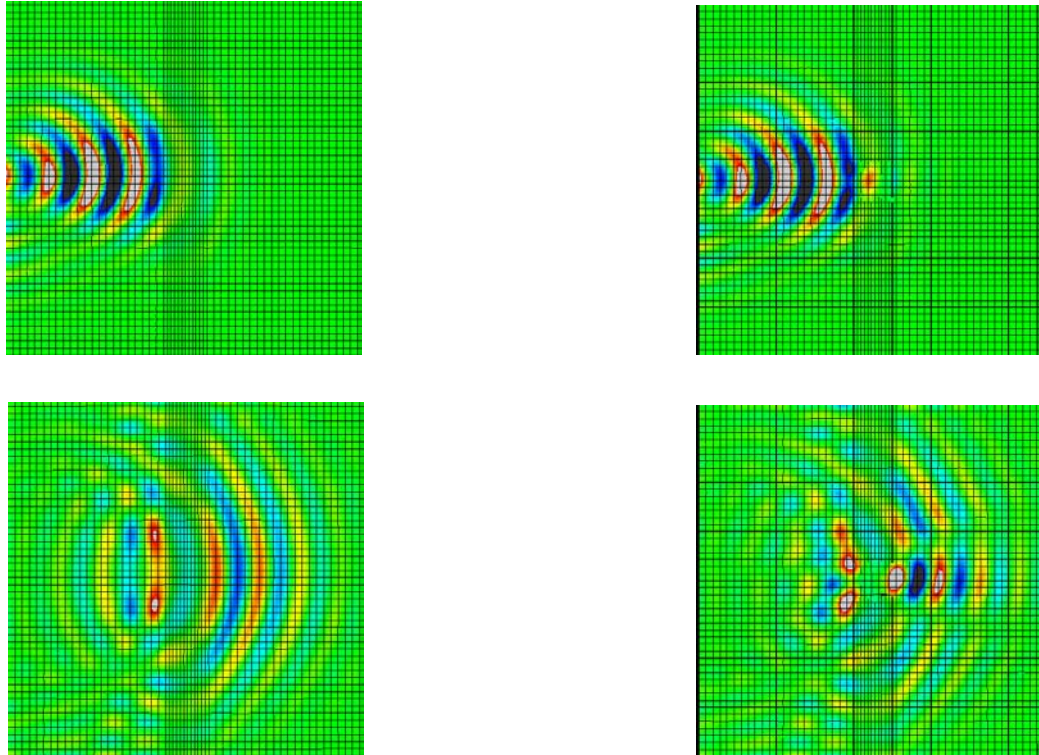
- Motivations for SHM within NRO OSL
 - hidden damage possible during manufacture and handling of spacecraft
 - lack of access to make quantitative measurements
 - detect/map extent of damage before and/or on the launch pad
 - facilitate launch/no-launch decisions
- Sensors/actuator optimization
 - increase reliable, robustness, signal strength of sensor/actuator
 - more efficient sensing schemes (architecture)
 - damage evaluation algorithms in MATLAB
 - large set of simple test results to compare, confirm, and tune
- Sandwich structure testing
 - test sensors/algorithms on more complex geometries
 - observe effects of various core densities and thickness
 - observe effects of disbonds, delams and gaps
 - continue to update algorithms supported by finite element analysis

Lamb Wave Methods

- Form of elastic perturbation that propagates in a solid medium
 - actuation parameters determined from governing equations
 - excite A_0 wave for long travel distances and to minimize clutter
- Damage can be identified in several ways
 - group velocity approximately $\propto (E/\rho)^{1/2}$, damage slows down waves
 - reflected wave from damage can be used to determine locations
- Research uses piezoelectric actuators/sensors to detect energy present in transmitted and reflected waves, builds off prior research



Effect of Damage on Lamb Waves



- Figure on left shows FEA results for stiffened plate without damage
- Figure on right shows FEA results for rib with 25 mm disbond
- Reduced stiffness in damaged region causes slower propagation
- Disbond yields fringe pattern in both reflected and transmitted wave

Sensors Material Analysis

- Use 3-1 piezoelectric coupling properties to output an open circuit voltage in response to strain wave
- Desirable attributes
 - maximize $\frac{k_{31}^2}{d_{31}(1-k_{31}^2)}$ where d_{31} is the 3-1 piezoelectric “strain” coefficient and k_{31} is the 3-1 coupling coefficient
 - minimum stiffness to maximize strain of wave passing through it
 - length of $(1 + n / 2) * \lambda$ where λ is the wavelength and $n = 0, 1, 2, 3, \dots$
 - capacitance such that 1 M Ω (oscilloscope impedance) appears as an open circuit to the sensor

Sensors Material Comparison

Material	k_{31}	d_{31}	g_{31}	Y_{11}^D	$ (k_{31})^2 / (d_{31} (1 - (k_{31})^2)) $
	(-)	(p m / V)	(mV m / N)	(GPa)	V / (mm $\mu\epsilon$)
PZT-7A	-0.300	-60	-16.2	104	1.65
EBL#5	-0.300	-60	-16	103	1.65
EBL#1	-0.360	-127	-10.7	106	1.17
EBL#7	-0.330	-107	-10.9	104	1.14
EBL#4	-0.310	-95	-10.5	110	1.12
PZT-8	-0.350	-127	-12.2	89	1.10
PZT-4	-0.340	-125	-10.6	91	1.05
EBL#9	-0.340	-135	-10.5	92	0.97
PZT-7D	-0.300	-112	-9.6	94	0.88
PZT-5R	-0.385	-200	-11.5	75	0.87
EBL#2	-0.360	-173	-11.5	76	0.86
PZT-5B	-0.380	-210	-10.1	79	0.80
PZT-5A	-0.343	-177	-11.1	71	0.75
EBL#23	-0.440	-320	-9	79	0.75
PZT-5J	-0.375	-230	-9.8	73	0.71
EBL#3	-0.380	-262	-8.6	75	0.64
PZT-5H	-0.375	-264	-8.9	69	0.62
EBL#6	-0.370	-260	-9.8	57	0.61
PZT-5M	-0.370	-270	-7.6	78	0.59
EBL#25	-0.300	-179	-11	49	0.55
PZT-5K	-0.380	-323	-6.9	73	0.52
PT2/PC6	-0.030	-3	-2.1	135	0.30

- Chart compares figure of merit for available PZT
- Separate analysis performed for PVDF
- Candidate materials which were selected to test broad range
 - EBL#5
 - EBL#1
 - EBL#2
 - EBL#23
 - EBL#3

Actuator Material Analysis

- Uses 3-1 piezoelectric coupling properties to output a strain wave in response to voltage

- Desirable attributes

- maximize the strain per volt induced in the structure, $P=2\pi fCV^2$

- maximize $\frac{e_{31}^P}{(c_{11}^P + c_{12}^P)h_P + (Q_{11} + Q_{12})h_S}$ where e^P is the planar piezoelectric “stress” coefficient, h_P and Q are the thickness and stiffness of the actuator, and h_S and c^P are the thickness and stiffness of the structure

- minimize the power delivered by the function generator by minimizing the admittance $\varepsilon_{33}^P \left(\frac{1}{h_P} + \frac{2c_{11}^P (k^P)^2}{(c_{11}^P + c_{12}^P)h_P + (Q_{11} + Q_{12})h_S} \right)$

where k^P is the planar coupling coefficient and ε^P the planar permittivity

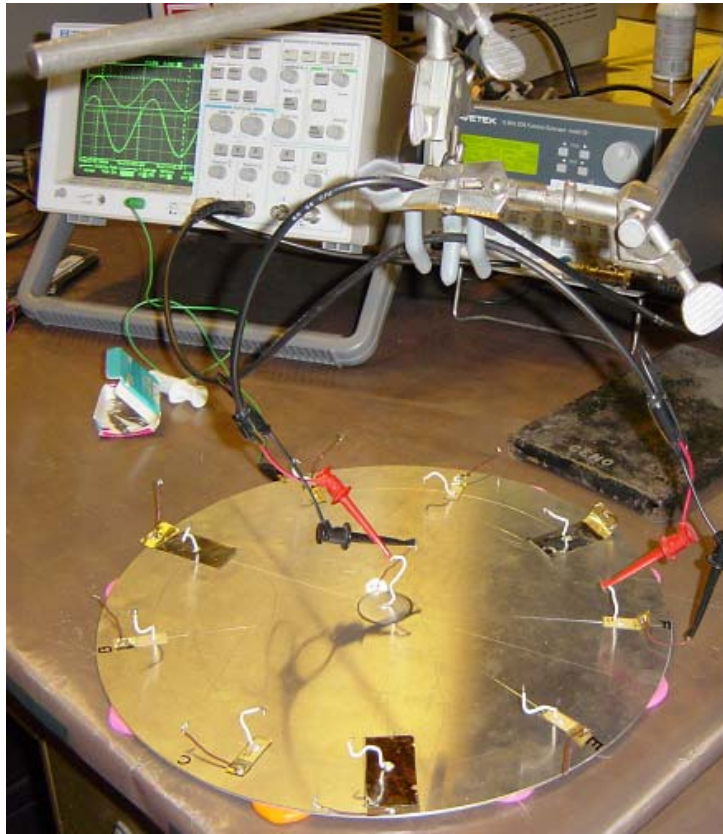
- resonant actuators also considered, but low frequencies required large dimensions (3-4” for 25 kHz) and had narrow range (250 Hz PZT-5A)

Actuator Material Comparison

Material	k_P	s_{11}^E	s_{12}^E	σ^P	ϵ_{33}^P	e_{31}^P
	(-)	(p m ² / N)	(p m ² / N)	(-)	(nF/m)	(N / m V)
EBL#23	0.750	15.7	-4.9	0.31	14.7	-29.6
PZT-5K	0.650	16.0	-5.1	0.32	29.6	-29.5
PZT-5M	0.630	15.0	-4.7	0.31	21.5	-26.1
EBL#3	0.640	15.6	-4.6	0.29	18.0	-23.9
PZT-5H	0.635	16.9	-5.1	0.30	17.4	-22.4
PZT-5J	0.630	16.0	-4.7	0.29	14.1	-20.3
PZT-5B	0.640	14.7	-4.3	0.29	12.3	-20.3
EBL#6	0.630	20.3	-6.3	0.31	14.7	-18.6
EBL#25	0.630	22.3	-12.2	0.55	9.6	-17.7
EBL#9	0.600	12.3	-4.4	0.36	8.2	-17.1
PZT-5R	0.630	15.7	-4.0	0.25	10.9	-17.1
EBL#2	0.620	15.1	-4.9	0.33	9.4	-17.0
PZT-5A	0.600	16.1	-5.6	0.35	9.7	-16.8
EBL#1	0.600	10.8	-3.0	0.28	7.4	-16.3
PZT-4	0.580	12.4	-3.9	0.31	7.6	-14.7
EBL#7	0.560	10.8	-3.3	0.31	6.7	-14.3
PZT-7D	0.510	11.8	-3.6	0.31	8.4	-13.7
EBL#4	0.520	10.1	-2.9	0.29	6.8	-13.2
PZT-8	0.520	12.8	-1.2	0.09	6.8	-11.0
EBL#5	0.520	10.6	-3.6	0.33	2.7	-8.5
PZT-7A	0.510	10.6	-3.3	0.31	2.6	-8.2
BT	0.260	7.8	-2.6	0.33	9.1	-8.1

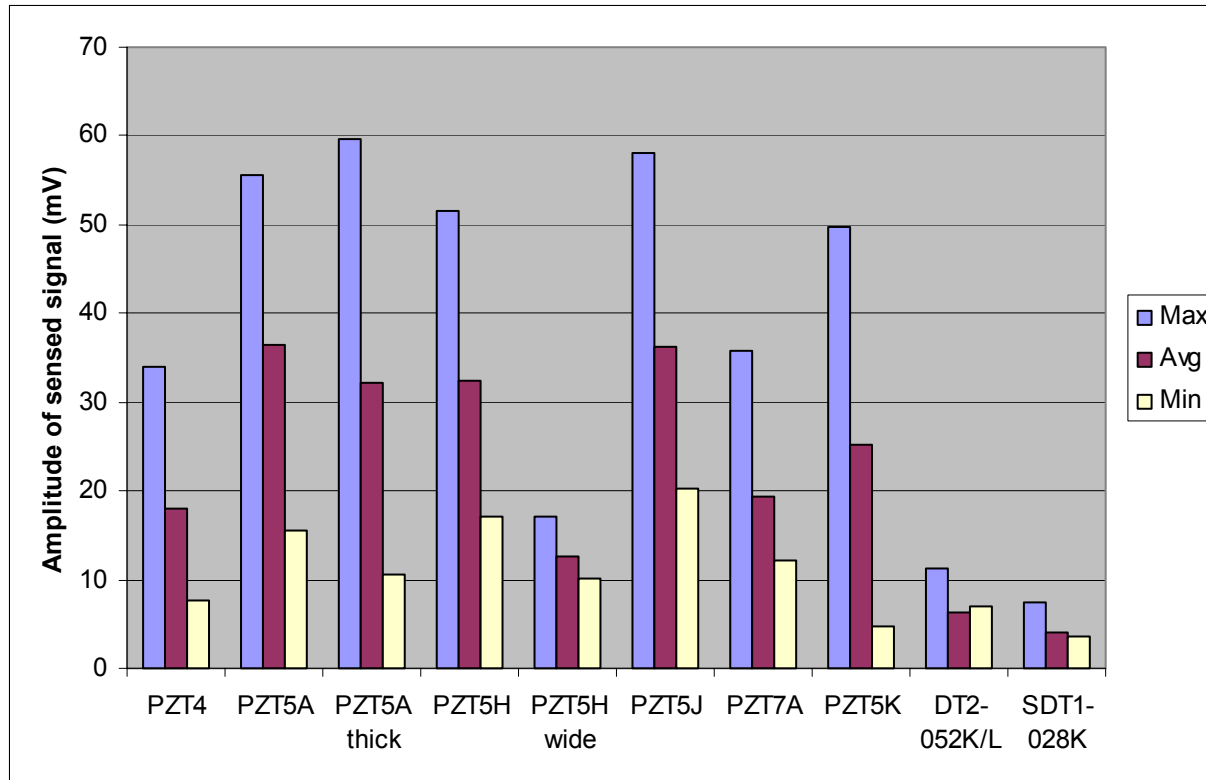
- Chart compares figure of merit for available PZT
- Separate analysis performed for resonant actuators
- Candidate materials which were selected to test broad range
 - EBL#23 (disk)
 - EBL#3
 - EBL#2
 - EBL#1 (disk)
 - EBL#5

Sensors/Actuator Material Testing



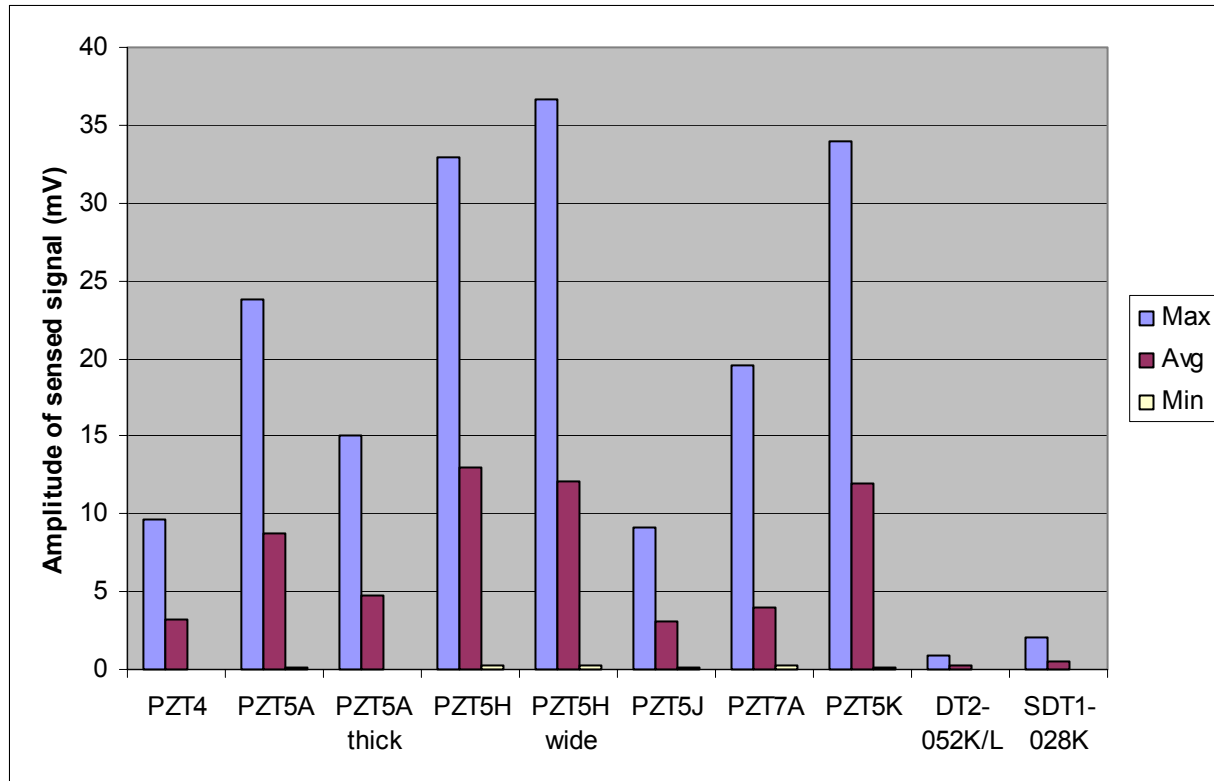
- Sensors bonded to circular Al plate
 - EBL#5 (PZT-7A) - 0.5x0.25x.01", 1.0x0.25x.01"
 - EBL#23 (PZT-5K) - 0.5x0.25x.01"
 - EBL#3 (PZT-5H) - 0.5x0.25x.01", 0.5x0.5x.01"
 - EBL#2 (PZT-5A) - 0.5x0.25x.01", 0.5x0.25x.02"
 - EBL#1 (PZT-4) - 0.5x0.25x.01"
 - DT2-052K/L PVDF
 - SDT1-028K PVDF
- Actuator disk in center
 - EBL#23 (PZT-5K) 0.5"(diameter)x0.01"
 - EBL#1 (PZT-4) 0.5"(diameter)x0.01"
- Tests performed
 - actuated from 1 kHz to 250 kHz
 - 20 V peak to peak
 - duplicates tested for each on separate plates
 - tests also performed in reverse

Sensors Material Results



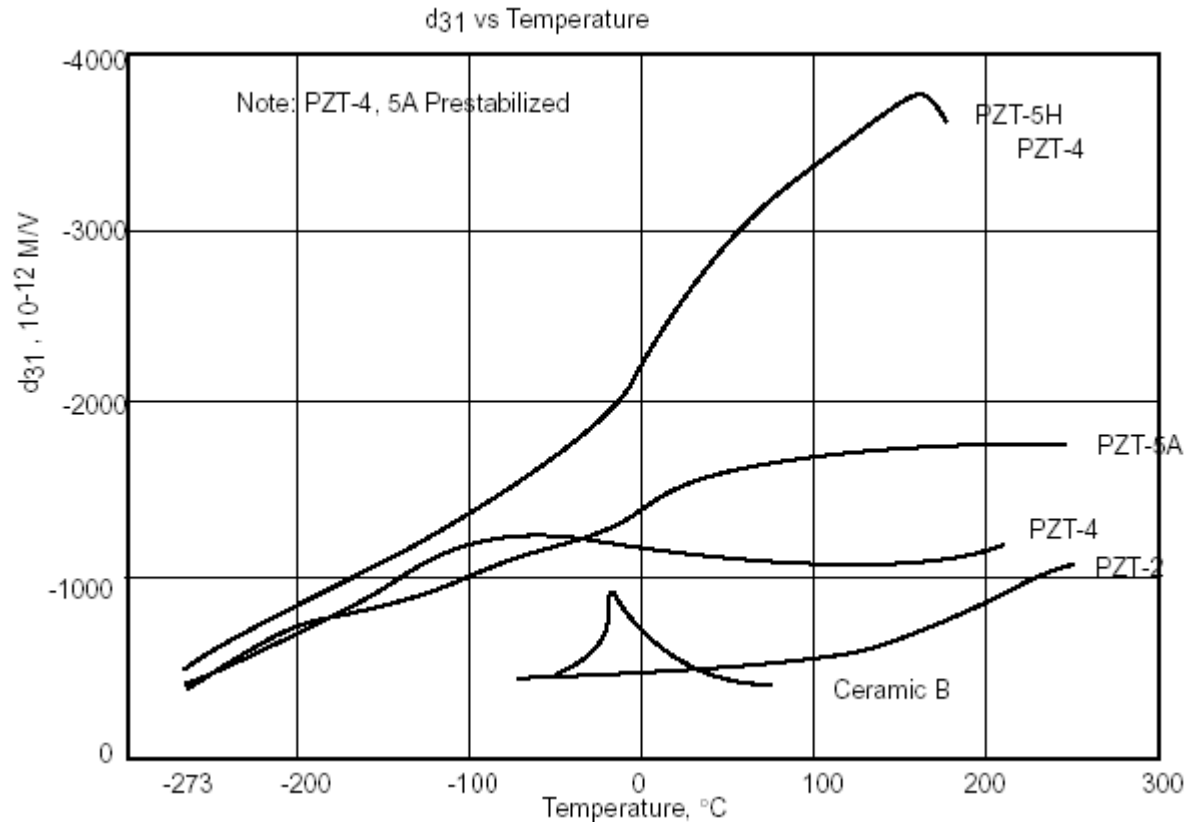
- PZT-5A, PZT-5H, PZT-5J, PZT-5K all comparable maximums
- PZT-5A and PZT-5J have highest means and minimums
- PZT-5A selected because of bandwidths of maximum peaks

Actuator Material Results



- PZT-5H and PZT-5K have highest amplitudes, PZT-5A close
- Overall averages were lower due to poor center sensor
- PZT-5A selected due to better actuation temperature stability

Temperature Stability



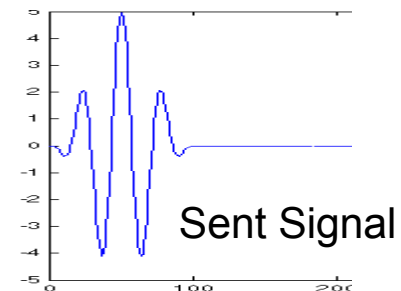
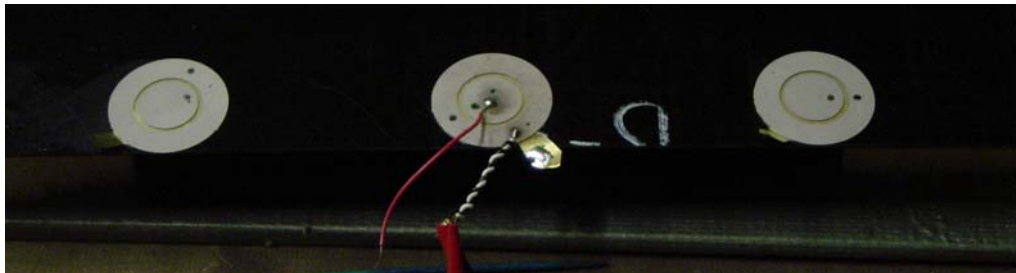
- PZT-5A has the best temperature stability of PZT materials
- PZT-5H has worst stability of PZT materials
- PZT-5K has comparable thermal properties to PZT-5H

Electrical/Mechanical Connections

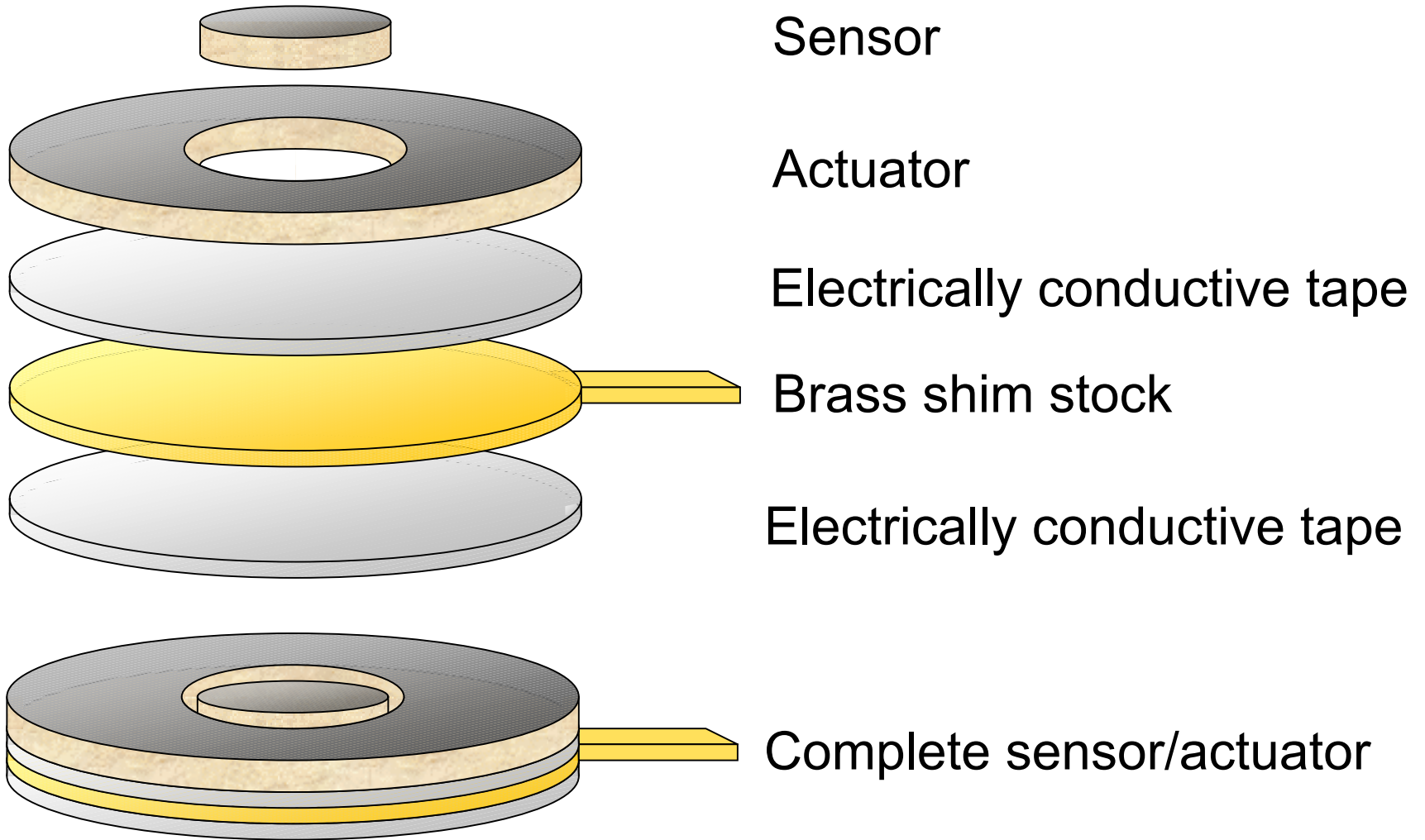
- Electrical connections
 - provide an electrical path to the underside of the piezoelectric wafers
 - minimize in-plane stiffness E^*t to maximize actuation (consider tearing)
 - reasonable through-thickness conductivity (resistance less than 1Ω)
- Mechanical connections
 - adhere piezoelectric wafer assembly to the structure
 - low application temperature, removable without damaging the structure
 - uniform thickness to reduce variability in surface mounting
 - must minimize G/t to maximum actuation
- Brass alloy 260 chosen for bottom electrode
 - 1 mil. thick shim stock used for conductor
 - 81% less stiff than copper shim used previously
- 3M 9703 electrically conductive double-sided tape chosen
 - used to adhere to brass and structure, non-conductive version available
 - 2 mil. thick chosen for adhesive
 - smoother and more repeatable than Ag epoxy

Piezoelectric Wafer Dimensions and Waveforms

- Actuator and sensor lengths
 - chosen to be 0.5” based upon equations for 15 kHz actuation
 - could be either length or diameter
- Actuator and sensor configuration
 - concentric disk/ring chosen for sensor/actuator, common ground
 - experiments demonstrated highest amplitudes with this setup
 - yields less electrical noise than “self-sensing” concepts
- Optimal actuation waveform
 - 15kHz chosen based on previous work
 - 3.5 sine waves w/Hanning window, will also collect data for 5.5 waves



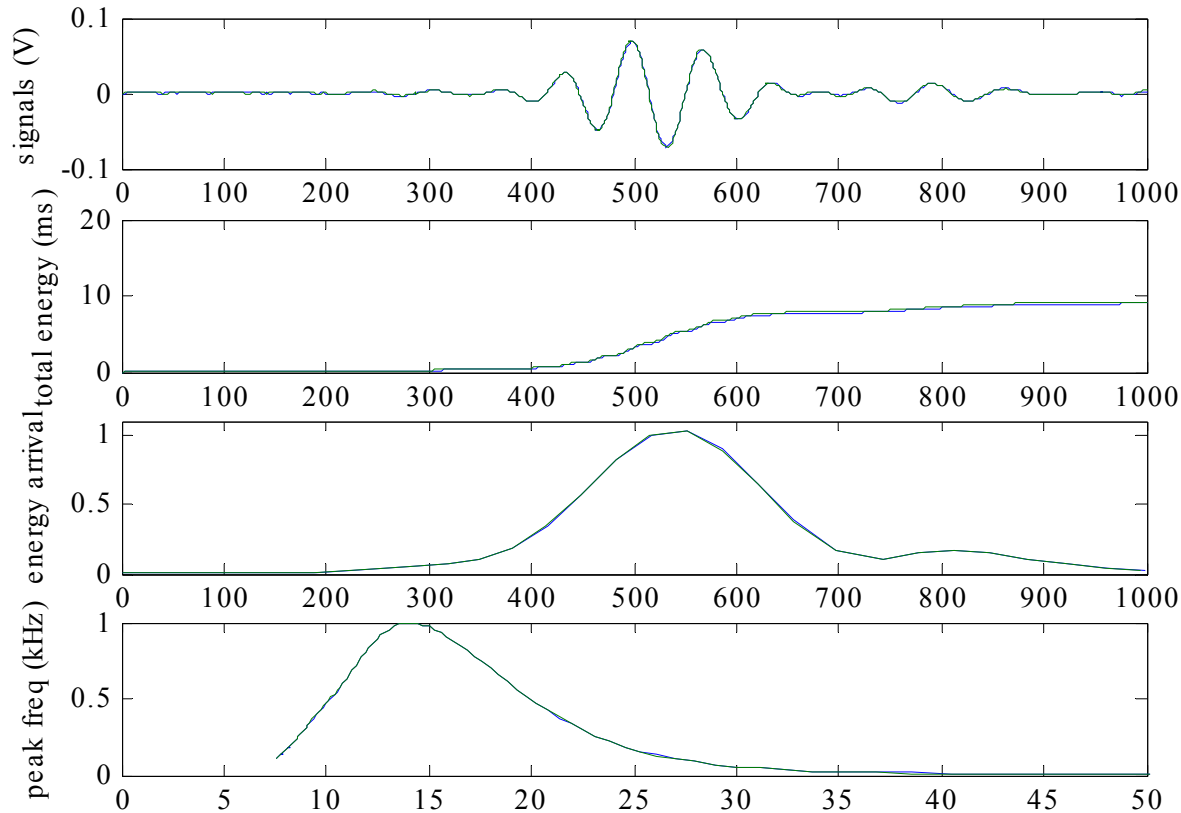
Actuator/Sensor Schematic



Data Reduction Procedure

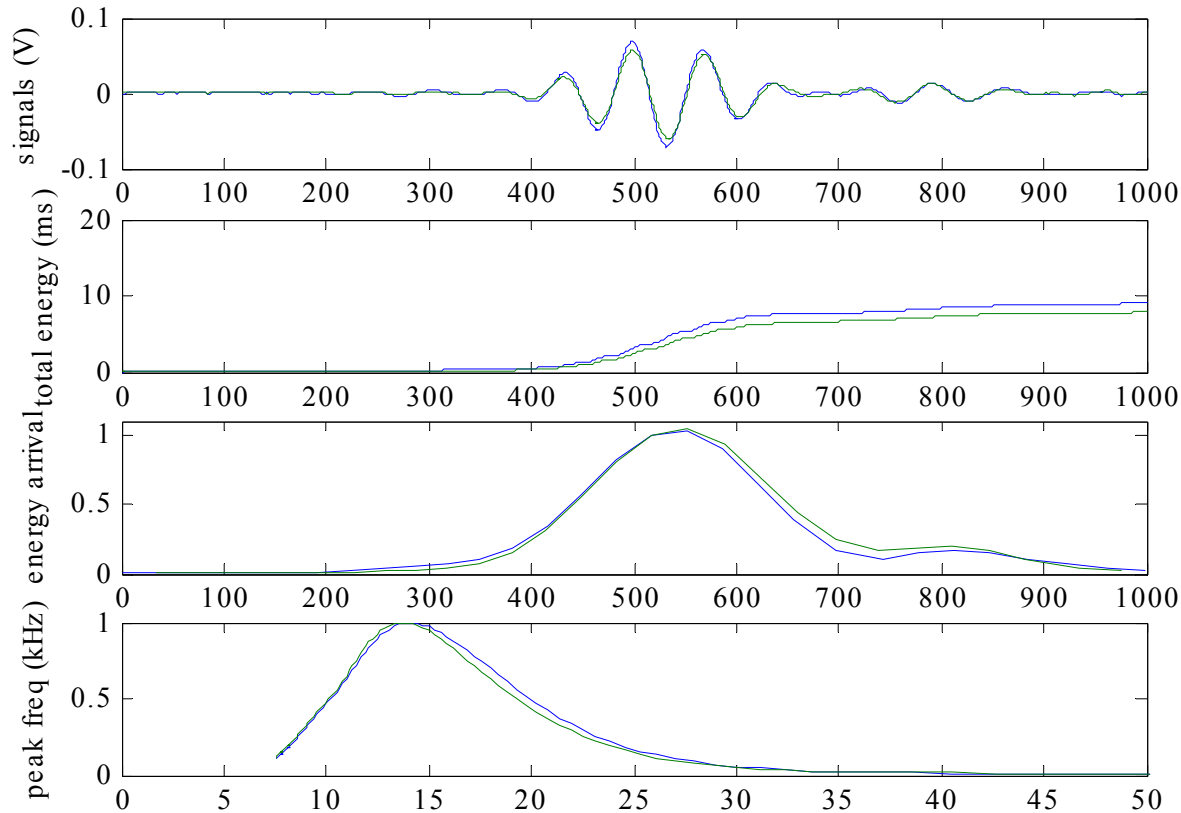
- Procedure developed within Matlab to reduce data
 - bandpass filter designed to remove low frequency drift and high frequency electrical noise without affecting signal shape
 - perform wavelet decomposition using Morlet mother wavelet to breakdown signal energy distribution between 7.5-50 kHz
 - plot *integrated voltage over time* yielding total received energy to determine *presence and severity* of damage
 - plot *normalized wavelet energy at driving frequency* of 15 kHz to determine time of arrival thus *damage location*
 - plot *normalized energy received for across wavelet spectrum* to determine *type of damage*
 - need 4 sets of plots: transmitted & reflected for 2 locations
- Need more consistent signals from new experiments to refine algorithms for automatic determination of damage

Experimental Results – Controls I



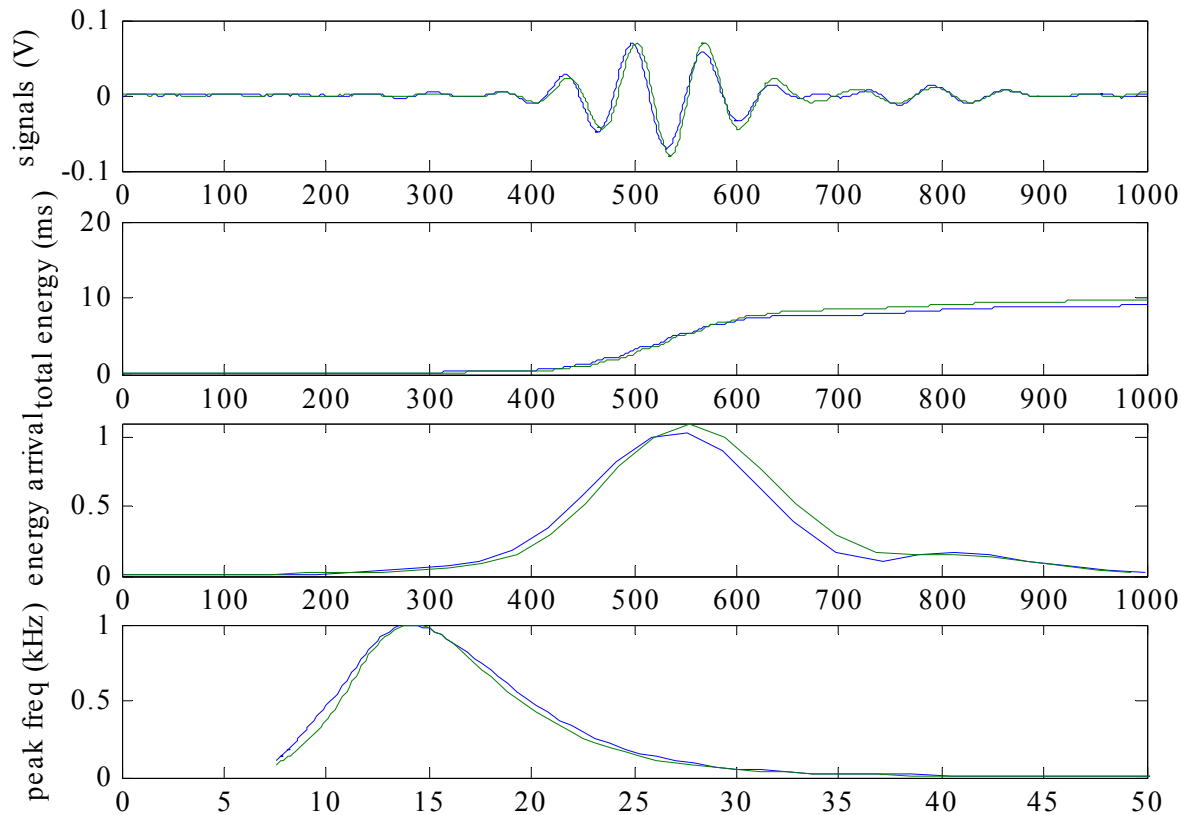
- Highly reproducible signal between same set of actuators and sensors tested several times

Experimental Results – Controls II



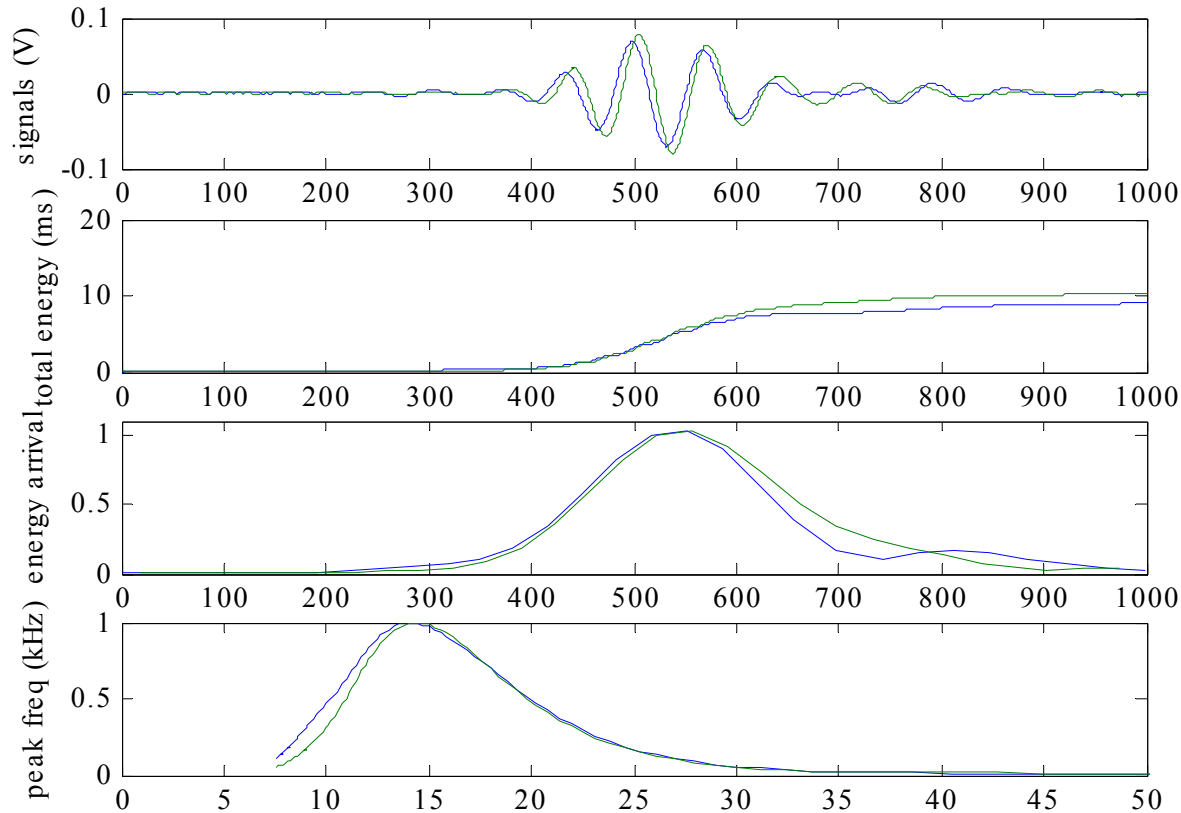
- Signal shape remains unchanged when propagating in reverse direction, other metrics remain similar

Experimental Results – Controls III



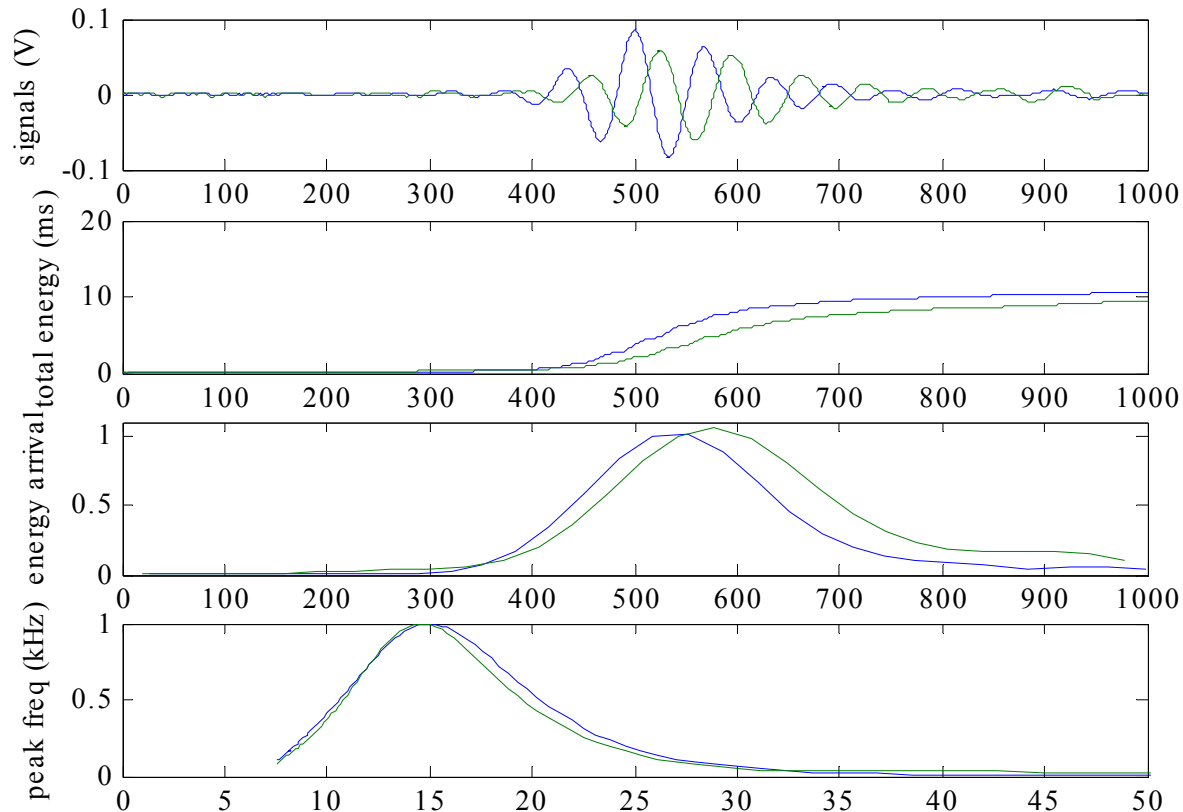
- Similar response across several different pairs of equally spaced actuators/sensors on same plate

Experimental Results – Controls IV



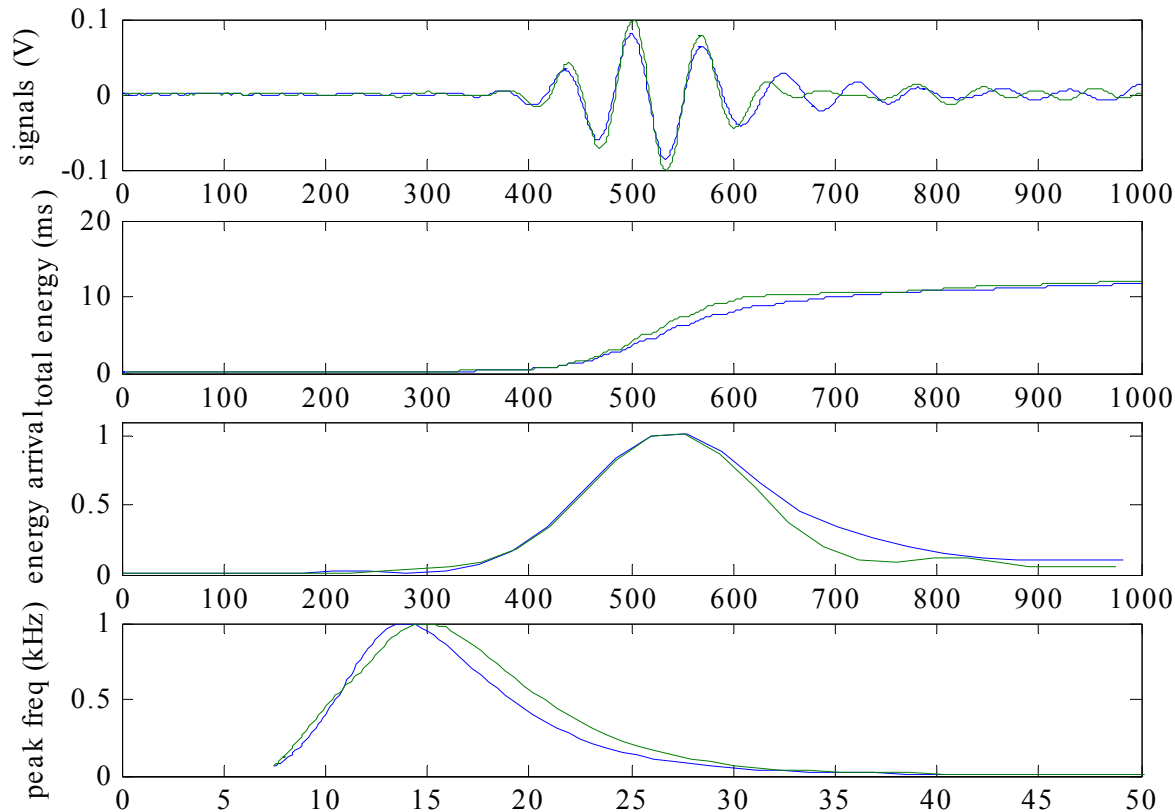
- Similar response between pairs of actuators/sensors located on several undamaged plates

Experimental Results – Delamination



- Delaminated signal is time-lagged, and has slightly lower energy content. Frequency bandwidth remains similar

Experimental Results – Microcracks



- Some matrix cracking caused a slight time delay, less tail energy and a small shift to a higher frequency bandwidth

Conclusions

- **Optimized setup** has **increased signal strength** nearly a factor of 4 over the previous research configuration
- **New decomposition algorithm** appears to work well with new data for transmitted wave, **eliminate subjectivity**
- **Undamaged response** is very **reliable/reproducible**
- Controlled damage does not have significant effect on most parameters, however voltage signal is lagged
- Reflected signal not yielding much information thus far
 - need to perform further analysis, maybe look at other frequencies
 - could affect ability to pinpoint damage location
- Will continue to collect more data to refine algorithm

Future Research

- Collect data on several plate specimens to refine algorithms
- Collect data for beam specimens with various core E and t's
- Continue studies on other potential detection methods
 - acoustic emission
 - eddy current
- Research focusing on other SHM components
 - wireless data acquisition and signal propagation
 - powering devices
- Increase complexity of tests
 - test on built up section
 - test in service environment (natural, mechanical, electrical noise)
 - use multiple sensing methods at once to increase reliability
 - integrate multiple SHM components